The effect of magnetic islands on tokamak diverters

Alkesh Punjabi1, Allen Boozer2

[1]Hampton University, Hampton, VA 23668, USA

[2]Columbia University, New York, NY 10227, USA

ABSTRACT: Divertors are required for handling the plasma particle and heat exhausts on the walls in fusion plasmas. Relatively simple methods are developed to study the plasma loss time and the interception pattern of the escaping plasma in divertor tokamaks using the field line Hamiltonian. The effects of the nonideal spiraling on the loss time and size of the footprint are studied. The DIII-D tokamak is chosen for the study. The complicated shape of the magnetic surfaces in the DIII-D is analytically represented by the equilibrium generating function. The surface that intercepts the escaping plasma is a plane orthogonal to the line from O-point to the X-point. The magnetic perturbation has mode numbers $(m,n) = (3,1) + (4,1)$. The resonant perturbation produces islands and stochastic regions. The plasma particles start on the last good surface and on a good surface roughly midway between the last good surface and magnetic axis. Scaling of the loss time and the size of the footprint with the nonideal spiraling effects are estimated.

The DIII-D map is used here as a precursor to the study of effect of magnetic islands on stellarator diverters. Much of the importance of the study is island diverters for stellarators. The approach and results here could also be important for tokamaks with non-axisymmetric perturbations. The DIII-D map just represents a typical tokamak divertor problem.

Outside of the last confining magnetic surface, field lines escape to the walls after a number of toroidal transits. The rate of direct loss of field lines is $\nu_d(x)$, where $1/\nu_d$ is the number of toroidal transits required for a field line to reach the wall when started a distance x outside the last confining magnetic surface. The artificial spiraling constant, D_s, is a velocity in the x direction. It is the distance a field line moves in x direction per toroidal transit. What will be shown is that when the rate of direct field line losses, $\nu_d(x)$, increases linearly with x, then the number of toroidal transits that are required for a field line to escape is $\tau_\ell \propto 1/D_s^{1/2}$ and when $\nu_d(x)$ increases cubically with x, then $\tau_\ell \propto 1/D_s^{3/4}$.

Assume a simulation is made by steadily introducing field lines at $x = 0$ at the rate Γ_0. The steady-state solution for field lines spiraling out and being lost to the walls is

$$\frac{d\Gamma}{dx} = -\dot{n}_d(x); \tag{1}$$

$$\Gamma(x) = n(x)D_s; \tag{2}$$

$$\dot{n}_d(x) = \nu_d(x)n(x), \tag{3}$$

where the total number of field lines in the steady-state system is $N = \int_0^\infty n(x)dx$. The loss time is defined as $\tau_\ell \equiv N/\Gamma_0$.

A characteristic distance is

$$\Delta(x) \equiv \frac{D_s}{\nu_d(x)}, \text{ so} \tag{5}$$

$$\Gamma(x) = \Delta(x)\dot{n}_d(x), \text{ and} \tag{6}$$

$$\tau_\ell = \frac{\int_0^\infty n(x)dx}{\int_0^\infty \dot{n}_d(x)dx}. \tag{7}$$

Equation (1) implies $d(\Delta\dot{n}_d)/dx = -\dot{n}_d$, so

$$\dot{n}_d \propto e^{-\sigma(x)}; \tag{8}$$

$$\sigma(x) \equiv \int_0^x \frac{1 + d\Delta/dx}{\Delta} \tag{9}$$

$$= \ln(\Delta/\Delta_0) + \int_0^x \frac{1}{\Delta}dx. \tag{10}$$

The implication is that

$$\dot{n}_d = \frac{c_0}{\Delta}e^{-\zeta(x)}; \tag{11}$$

$$\zeta(x) \equiv \int_0^x \frac{1}{\Delta}dx \tag{12}$$

$$= \frac{u(x)}{D_s}, \text{ where} \tag{13}$$

$$u(x) \equiv \int_0^x \nu_d(x)dx. \tag{14}$$

where c_0 is a constant. It will be assumed that $\nu_d(x)$ increases sufficiently rapidly with x that $\zeta(x \to \infty) \to \infty$, which ensures all field lines are lost in the region $x > 0$. Then,

$$\int_0^\infty \dot{n}_d(x)dx = c_0, \tag{15}$$

$$\int_0^\infty n(x)dx = \frac{c_0}{D_s}\int_0^\infty e^{-\zeta(x)}dx; \tag{16}$$

$$\tau_\ell = \frac{\int_0^\infty e^{-\zeta(x)}dx}{D_s} \tag{17}$$

$$= \frac{\int_0^\infty \exp\left(-\frac{u(x)}{D_s}\right)dx}{D_s}. \tag{18}$$

When the direct loss rate is proportional to distance, $\nu_d(x) = \nu'_0 x$ with ν'_0 a constant, $u(x) = \nu'_0 x^2/2$. Using $\int_0^\infty exp(-s^2)ds = \sqrt{\pi}/2$,

$$\tau_\ell = \sqrt{\frac{\pi}{\nu'_0 D_s}}. \tag{19}$$

When the direct loss rate is proportional to distance cubed, $\nu_d(x) = \nu'''_0 x^3/6$ with ν'''_0 a constant, $u(x) = \nu'''_0 x^4/24$. Using $\int_0^\infty exp(-s^4)ds = \Gamma(5/4) \approx 0.9064$,

$$\tau_\ell = \frac{\Gamma(5/4)}{D_s}\left(\frac{24D_s}{\nu'''_0}\right)^{1/4}. \tag{20}$$

The equilibrium genearting function (EGF) for the DIII-D is very complicated. The analytic representation of the DIII-D EGF in natural canonical coordinates (NCC) and the forward, backward, and continuous symplectic maps for the DIII-D in NCC are given in [1,2]. The form of the spiralling operator D_s is $r \rightarrow r+(0.9+2R_N)D_s$. R_N is a random number in the interval (0,1].

For the case of lines starting on a good surface midway between the O-point and the X-point, the maplitude of perturbation is δ=5E-4. In this case the loss time scales as $D_s^{-3/4}$ for both the forward and the backward lines. See Figs. 1-2. The area of the forward and backward footprint scales as $D_s^{1/4}$. See Figs. 3-4. These results are consistent with the prediction above when the direct loss is proportional to distnce cubed, Equation (20).

For the case of lines starting on the LGS, the maplitude of perturbation is δ=5E-3. In this case the loss time scales as $D_s^{-1/2}$ for both the forward and the backward lines. See Figs. 5-6. The area of the forward and backward footprint scales as $D_s^{1/2}$. See Figs. 7-8. These results are consistent with the prediction above when the direct loss is proportional to distnce, Equation (19).

Simple model is developed to predict the loss time and the area of of the footprint of plasma particles in tokamaks. This model is applied to the DIII-D using the DIII-D map for the two cases of the lines atrating midway between the O-point and X-point and on the LGS in the DIII-D. The results of the computation are consistent with the predictions of the model.

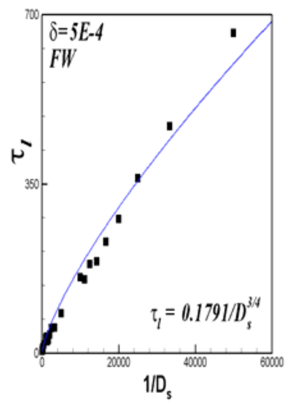

Fig. 1. Loss time as a function of spiraling coefficient for forward lines when lines start midway between O-point and X-point.

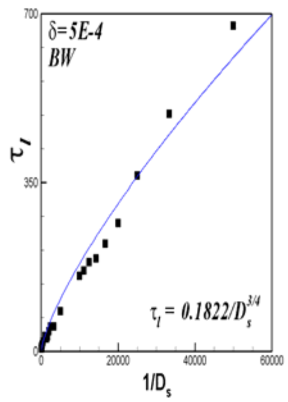

Fig. 2. Loss time as a function of spiraling coefficient for backward lines when lines start midway between O-point and X-point.

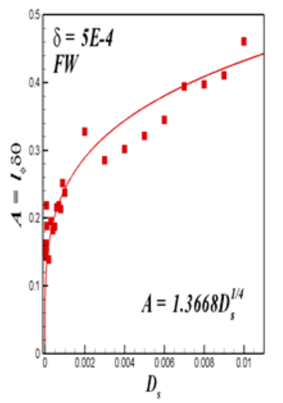

Fig. 3. The area of the footprint as a function of spiraling coefficient for forward lines when lines start midway between O-point and X-point.

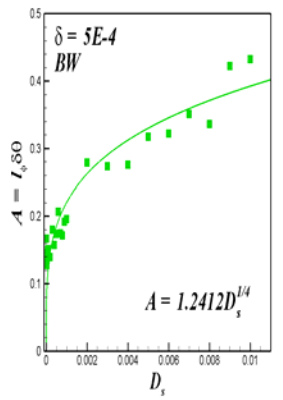

Fig. 4. The area of footprint as a function of spiraling coefficient for backward lines when lines start midway between O-point and the X-point.

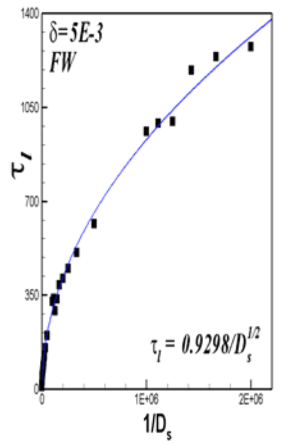

Fig. 5. Loss time as a function of spiraling coefficient for forward lines when lines start on the LGS.

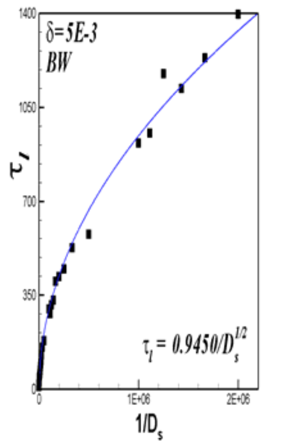

Fig. 6. Loss time as a function of spiraling coefficient for backward lines when lines start on the LGS.

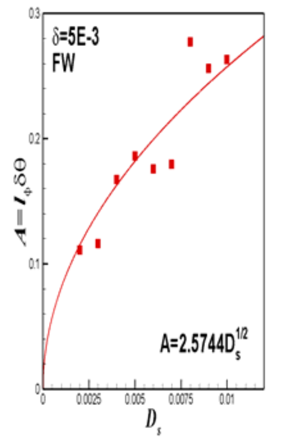

Fig. 7. The area of the footprint as a function of spiraling coefficient for forward lines when lines start on the LGS.

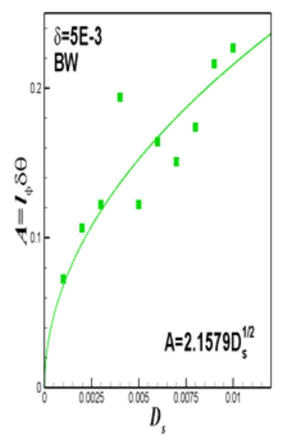

Fig. 8. The area of footprint as a function of spiraling coefficient for backward lines when lines start on the LGS.

This work is supported by the US DOE grants DE-FG02-01ER54624 and DE-FG02-04ER54793 to Hampton University and DE-FG02-95ER54333 to Columbia University. This research used resources of the NERSC, supported by the Office of Science, US DOE, under Contract No. DE-AC02-05CH11231.

[1] A. Punjabi and H. Ali, Phys. Plasmas **15**, 122502 (2008)

[2] A. Punjabi, Nucl. Fusion **49**, 115020 (2009)